

Article

Multimodal Data Integration to Predict Severe Acute Oral Mucositis of Nasopharyngeal Carcinoma Patients Following Radiation Therapy

Yanjing Dong ¹ , Jiang Zhang ¹ , Saikt Lam ^{2,3}, Xinyu Zhang ¹, Anran Liu ¹, Xinzhi Teng ¹, Xinyang Han ¹ , Jin Cao ¹, Hongxiang Li ⁴, Francis Karho Lee ⁵, Celia Waiyi Yip ⁵, Kwokhung Au ⁵, Yuanpeng Zhang ⁶ and Jing Cai ^{1,2,7,*} 

¹ Department of Health Technology and Informatics, The Hong Kong Polytechnic University, Hong Kong SAR, China

² Research Institute for Smart Ageing, The Hong Kong Polytechnic University, Hong Kong SAR, China

³ Department of Biomedical Engineering, Faculty of Engineering, The Hong Kong Polytechnic University, Hong Kong SAR, China

⁴ Department of Radiology, Fujian Medical University Union Hospital, Fujian Medical University, Fuzhou 350000, China

⁵ Department of Clinical Oncology, Queen Elizabeth Hospital, Hong Kong SAR, China

⁶ Department of Medical Informatics, Nantong University, Nantong 226000, China

⁷ The Hong Kong Polytechnic University Shenzhen Research Institute, Shenzhen 518000, China

* Correspondence: jing.cai@polyu.edu.hk

Simple Summary: The acute oral mucositis (AOM) is a prevalent side effect of radiation therapy for nasopharyngeal carcinoma (NPC). Severe AOM could impair the survival and quality of life for NPC patients. Accurate method to predict the incidence of severe AOM can aid clinicians in adjusting the treatment plan to improve the outcomes for NPC patients. We integrated multimodalities, multi-omics and multi-regions data with two methods, integrate the original data or combine data after feature selection. The performance of models using each data integration method with different modalities, types of data and VOIs were analyzed. We developed a best-performing model with mean AUC at 0.81 ± 0.10 to predict the incidence of severe AOM for NPC patients following radiation therapy.

Abstract: (1) Background: Acute oral mucositis is the most common side effect for nasopharyngeal carcinoma patients receiving radiotherapy. Improper or delayed intervention to severe AOM could degrade the quality of life or survival for NPC patients. An effective prediction method for severe AOM is needed for the individualized management of NPC patients in the era of personalized medicine. (2) Methods: A total of 242 biopsy-proven NPC patients were retrospectively recruited in this study. Radiomics features were extracted from contrast-enhanced CT (CECT), contrast-enhanced T1-weighted (cT1WI), and T2-weighted (T2WI) images in the primary tumor and tumor-related area. Dosiomics features were extracted from 2D or 3D dose-volume histograms (DVH). Multiple models were established with single and integrated data. The dataset was randomized into training and test sets at a ratio of 7:3 with 10-fold cross-validation. (3) Results: The best-performing model using Gaussian Naive Bayes (GNB) (mean validation AUC = 0.81 ± 0.10) was established with integrated radiomics and dosiomics data. The GNB radiomics and dosiomics models yielded mean validation AUC of 0.6 ± 0.20 and 0.69 ± 0.14 , respectively. (4) Conclusions: Integrating radiomics and dosiomics data from the primary tumor area could generate the best-performing model for severe AOM prediction.

Keywords: multimodal data integration; radiomics; dosiomics; nasopharyngeal carcinoma; acute mucositis



Citation: Dong, Y.; Zhang, J.; Lam, S.; Zhang, X.; Liu, A.; Teng, X.; Han, X.; Cao, J.; Li, H.; Lee, F.K.; et al.

Multimodal Data Integration to Predict Severe Acute Oral Mucositis of Nasopharyngeal Carcinoma Patients Following Radiation Therapy. *Cancers* **2023**, *15*, 2032. <https://doi.org/10.3390/cancers15072032>

Academic Editors: Wei Wu and Trevor G. Bivona

Received: 23 February 2023

Revised: 21 March 2023

Accepted: 26 March 2023

Published: 29 March 2023



Copyright: © 2023 by the authors. Licensee MDPI, Basel, Switzerland. This article is an open access article distributed under the terms and conditions of the Creative Commons Attribution (CC BY) license (<https://creativecommons.org/licenses/by/4.0/>).

1. Introduction

Nasopharyngeal carcinoma (NPC) is a kind of malignant epithelial head and neck (H&N) cancer. It originates from the nasopharyngeal mucosal lining with high incidence in Southeast Asia [1]. Over 95% of NPC cases are non-keratinizing squamous cell carcinoma that is highly sensitive to radiation [2]. Radiotherapy with/without chemotherapy (CRT or RT, respectively) is the primary treatment for NPC patients to achieve disease control. Although advanced radiation strategies such as intensity-modulated RT (IMRT) are widely applied to reduce the recurrence rate of tumor with decreased radiation-induced side effects [3,4], radiation toxicity is still a trouble for NPC patients undergoing radiation therapy [5,6]. The radiation damages DNA and cellular components, which could cause mitotic cell death, apoptosis, and cytokine cascade in the human body. These cascades of events could eventually and inevitably lead to toxicity effects [7]. Most NPC patients suffer from dermatitis, mucositis, dysphagia, and xerostomia during and after RT/CRT. Among these acute toxicity effects, acute oral mucositis (AOM) is the most common painful symptomatic complication for NPC patients [8].

More than 60% of H&N patients have experienced AOM following RT-based anti-cancer therapies. Approximately 65% of these patients have developed severe AOM (\geq grade 3) [8]. The AOM is typically characterized by atrophy, swelling, erythema, and ulceration. It often impairs patients' functional status and quality of life (QoL) [9]. The soreness of AOM initially leads to open-mouth difficulty, which further causes decreased food and water intake, loss of weight, and systematic infection. Patients who have developed severe AOM with painful experiences would receive a reduced dose of chemotherapy. Some patients even tend to break the RT regime. Severe AOM can exacerbate the morbidity of patients, which may finally contribute to worsen QoL and increase mortality [10]. It therefore is necessary to analyze the critical contributors to the oral mucositis.

Previous studies have focused on analyzing one type of data, such as genetic data and clinical variables, for predicting severe AOM. Various factors have been identified to correlate with the incidence and severity of oral mucositis, for instance, genetic background [11,12], dose of RT [13,14], chemo-drugs [15–17], and nutritional status [18]. Among these factors, the dose of RT is a critical factor influencing the severity of AOM. Additional chemotherapy, especially with some AOM-associated agents, for instance, alkylating agents and antimetabolites, could exacerbate the events. Besides, AOM patients are more likely to have weight loss during the treatment scheme [19,20]. Saito et al. [20,21] reported that low BMI is a risk factor for severe AOM. Andy et al. [21] indicated that patients with advanced tumors are prone to experience AOM. Moreover, a recent two-stage genome-wide association study [12] showed that four single nucleotide polymorphisms (SNPs) might be correlated with acute mucositis. However, they failed to validate their results in the validation stage. Clinicogenomic variables alone are inadequate to accurately predict the incidence, correlations, and severity of AOM for NPC patients after RT.

In addition to the genomics information, contrast-enhanced computed tomography (CECT), magnetic resonance imaging (MRI), and dose files routinely acquire clinical data for NPC patients with RT plans [22,23]. Radiomics and dosiomics are two quantitative information-extraction methods to provide minable texture and dose-distribution information for clinical prognosis prediction. Traditional experiences have demonstrated that single or double sources of data had limited prediction power for acute AOM. Integration of complementary data from multiple types of datasets can lead to an intricate outcome than a simple summation of information [24]. Integration of multimodal data from multiple sources, for instance, clinical, radiomics, and dosiomics for NPC patients, has the potential to overcome the boundaries of conventional medical analysis [25–31]. Unfortunately, few studies have reported the possibilities of radiomics or dosiomics for AOM prediction [13,32,33]. To the best of our knowledge, there are no studies in the literature assessing whether the data fusion of multi-regions and multimodalities could enhance their capability of severe AOM prediction.

In this study, we aimed to analyze multimodal data, including clinical, radiomics, and dosiomics information, to predict the incidence of severe AOM in NPC patients following RT/CRT. The radiomics and dosiomics data were extracted from multi-regions related to RT treatment. These data were also extracted from multimodalities of images (CECT, contrast-enhanced T1-weighted, and T2-weighted MRI). In daily clinical practice, clinicians could benefit from adjusting treatment plans before RT for patients with a higher possibility of developing severe AOM to achieve personalized diagnosis and treatment.

2. Materials and Methods

Patient data. All patient data were retrospectively collected from NPC patients who underwent CRT or RT at Hong Kong Queen Elizabeth Hospital from 2012 to 2015. Informed consent of patients was waived due to the nature of the retrospective study. NPC patients were recruited based on the following inclusion and exclusion criteria. The inclusion criteria were: (1) NPC patients with pathological validation and absence of distant metastasis and co-existing tumors of other types at diagnosis, (2) patients treated with a total RT dose of 60–70 Gy, and (3) patients with a completed set of clinical, image, and radiation dosimetry data. The exclusion criteria were: (1) patients aged less than 18, (2) patients without original image or clinical data; and (3) patients for whom exact standard terminology criteria for adverse events (CTCAE) evaluation for AOM had not been recorded. Symptoms in grades 1 and 2 were defined as mild AOM, and grades 3 and 4 as severe AOM [34]. All the patients were negative of oral mucositis according to the CTCAE grading system before receiving radiation therapy.

Clinical variables included (1) treatment information: TNM stage, treatment, past health condition, allergy history, vision condition, hearing condition, and CTCAE evaluation for AOM and (2) demographic data: age, gender, body weight, height, body mass index (BMI), and smoking and drinking habits. All clinical variables were acquired one week before RT commencement, except the CTCAE evaluation results, which were recorded 4–5 weeks after RT commencement. The equation for BMI is defined as follows:

$$\text{Body mass index (BMI)} = \text{weight}/\text{height}^2 \quad (1)$$

Patients were maintained in a supine position during the imaging examination. Details of imaging acquisition are summarized in Tables A1 and A2.

Image pre-processing. In this study, the imaging pre-processing steps were based on our previous work [28] and are in accordance with the Image Biomarker Standardisation Initiative (IBSI) guidelines [35]. Specifically, (1) voxel size resampling: all images (CECT and MRI) were resampled to a voxel size of $1 \times 1 \times 1 \text{ mm}^3$; (2) volume of interest (VOI) re-segmentation: CECT images were re-segmented to confine the Hounsfield unit (HU) to (−150,180) to eliminate the non-soft tissue in the VOI; (3) image filtering: a Laplacian of Gaussian (LoG) filter with three levels of Gaussian radius parameter was used under fine (1 mm), medium (3 mm), and coarse (6 mm) scales; (4) quantization of gray levels: gray-level intensities of the images were fixed to 50 bins; and (5) inhomogeneity correction of image pixel value: N4B bias correction in the “N4 Bias Field Correction Image Filter” in SimpleITK (v1.2.4) was implemented, in particular, to MRI images.

Radiomics and dosiomics feature extraction. Feature extraction was performed using our in-house platform based on publicly available SimpleITK (v1.2.4) and PyRadiomics (v2.2.0) [36,37]. All VOIs were delineated by an experienced senior clinician [38]. The gross tumor volumes (GTVs) were contoured based on CECT with the assistance of MRI images.

Radiomics. The gross tumor volume of the NPC primary tumor (GTV_{np}) and the gross tumor volume of nodal lesions (GTV_n) were selected as the main VOIs for radiomics feature extraction. Features with or without LoG filters were both involved. All these features were extracted from CECT, contrast-enhanced T1 weighted (cT1WI), and T2 weighted (T2WI) images (for details, please refer to Figure 1). Meaning of each VOI for different image modalities were listed in Table 1.

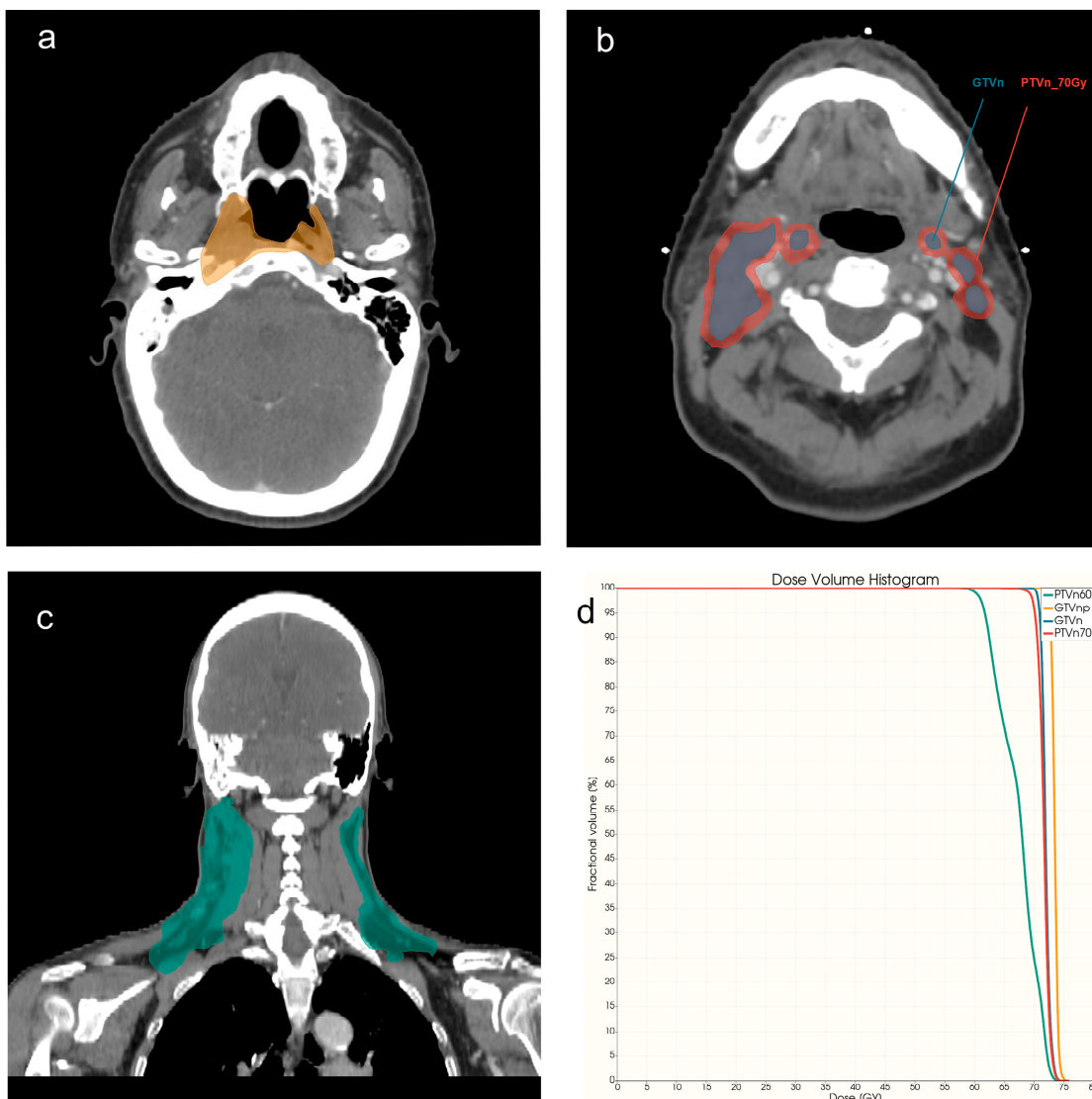


Figure 1. VOI examples for NPC patients with CECT examination. (a) Region of GTVnp (orange), axial view. (b) Region of GTVn (blue) and PTVn_70 Gy (red), axial view. (c) Region of PTVn_60 Gy (green), coronal view. (d) DVH curve of four VOIs.

Table 1. VOIs and image modalities.

| VOIs | Descriptions of VOI | Imaging Modalities/Images |
|-----------|--|---------------------------|
| GTVnp | Gross tumor volume of primary NPC tumor | CECT, cT1WI, T2WI, DVH |
| GTVn | Metastatic lymph nodes area | CECT, DVH |
| PTVn_70Gy | Regions of nodal planning target volume with the prescribed dose level of 70Gy | DVH |
| PTVn_60Gy | PTVn with the prescribed dose level of 60Gy | DVH |

Three categories of radiomics features were extracted: shape, first-order statistics, and texture features. The texture features can be further categorized into gray-level difference matrix (GLDM), gray-level cooccurrence matrix (GLCM), gray-level run-length matrix (GLRLM), gray-level size-zone matrix (GLSZM), and neighboring gray-tone difference matrix (NGTDM) classes.

Dosimetrics. Except for GTVnp and GTVn, the region of the high-dose nodal planning target volume (PTVn_70Gy) and region of the low-dose nodal planning target volume (PTVn_60Gy) were also added to the dosimetrics analysis (please refer to Figures 1 and A2 and Table 1 for more details).

Two-dimensional (2D) and three-dimensional (3D) dose–volume histograms (DVHs) of each studied VOI were extracted from dose files for dosimetrics feature extraction. All dosimetrics features were extracted based on Gabry et al.’s previous study [39]. Features that reflect dose distribution, for instance, mean dose, spatial dose gradient, and spatial dose spread were extracted accordingly. All the calculation algorithms have been listed in a previous publication by Buettner et al. [40].

Model development and evaluation. The statistical analysis, model training, and evaluation were conducted in Jupyter 6.4.12 and SPSS 25. The receiver operating characteristic (ROC) curve and area under the ROC curve (AUC) with 10-fold validation was performed to evaluate model performance. The CTCAE grade scale of patients in mucositis was dichotomized between severe AOM (grade ≥ 3) and mild AOM (grade ≤ 2) as the prediction endpoint. Patients were stratified based on CTCAE grade to training and testing groups at a 7:3 ratio (details in Figure 2).

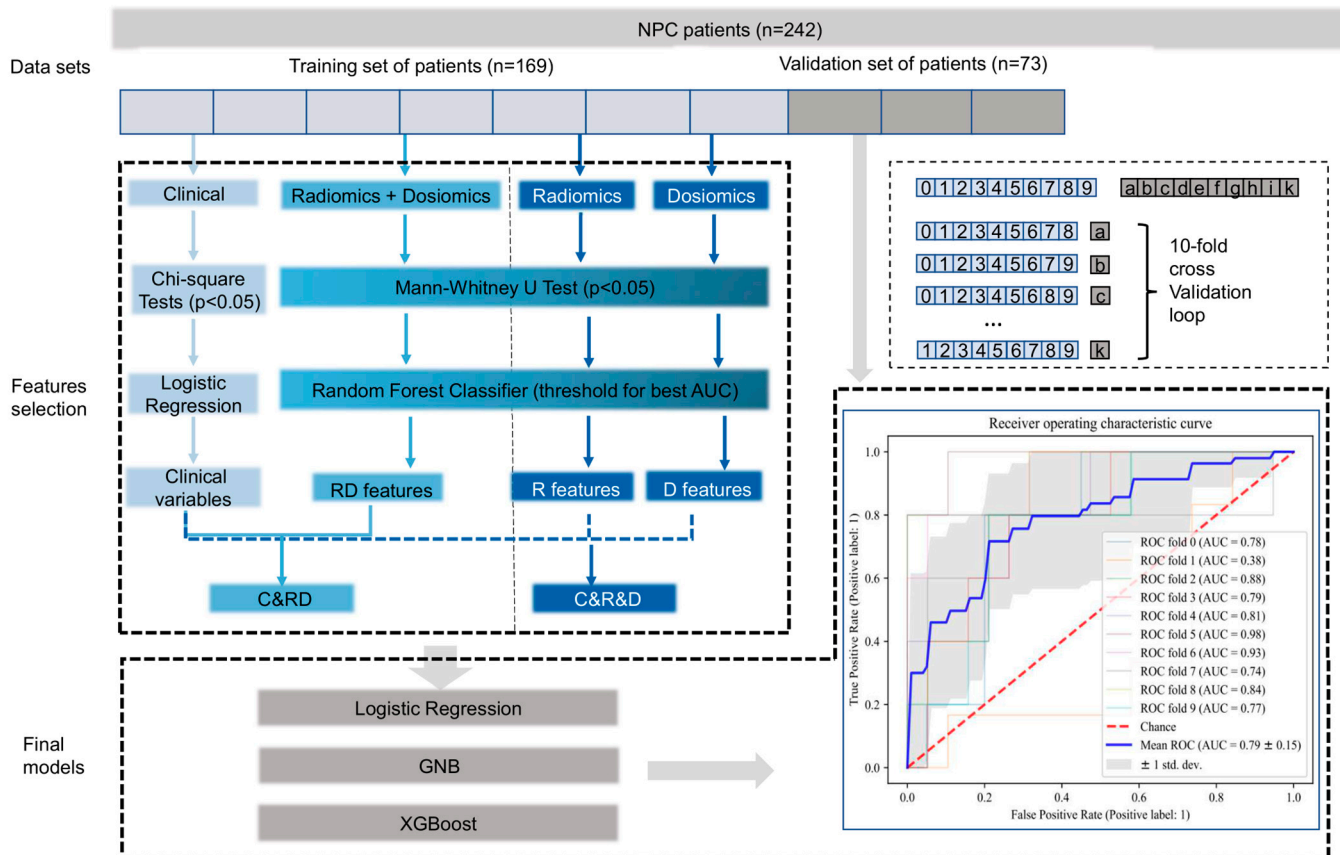


Figure 2. Scheme of feature selection and modeling. Training and validation sets were separated before data analysis. The training set of data was used for feature selection. The validation set of data was used for model evaluation. To further manipulate the numerical and categorical data, reduce the interactions, and solve the collinearity problems, random forest (RF) selection was applied for radiomics, dosimetrics, and integrated data. Three linear or non-linear models were developed with independent validation data sets with selected features. The area under the curve (AUC) was set as the main evaluation method for the model performance.

Single-modal models. The data sources for single-modal models were restricted to single modality of data (radiomics, dosiomics, or clinics), single modality of imaging (CECT, cT1WI, T2WI, and DVH), and single region of patients (GTVnp, GTVn, PTVn_60Gy, and PTVn_70Gy). Each single data set had two steps in this stage: (1) feature selection and model training in the training group set and (2) AUC evaluation in validation groups.

For clinical data, chi-square and Mann–Whitney U tests were employed for binary and non-binary variables for univariate analysis. p values < 0.05 was considered to be statistically significant. All radiomics and dosiomics data were standardized with the MinMax scaler before selection. For radiomics and dosiomics data, we first identified significant features between severe and mild AOM patients in the training set with Mann–Whitney U tests. After that, random forest (RF) was used to rank the importance of the significant features considering both feature interactions and nonlinearities. The optimal feature number was set according to the best RF training model score. Three models, including logistic regression (LR), Gaussian Naïve Bayes (GNB), and extreme gradient boosting (XGBoost), were applied to evaluate the combined predictive value of these selected features in the independent validation set. All VOIs data were analyzed separately at the single model stage.

Multimodal data integration. Clinical data after multivariate analysis (LR) with p value < 0.05 were selected for data integration. Dosiomics and radiomics data from different VOIs and image modalities were integrated with two methods: (1) dosiomics and radiomics data were combined together before feature selection and (2) the features selected from the RF model were merged and directly combined without a further feature-selection step (please refer to Figure 2 for more details). All the data-integration methods are listed in Table 2.

Table 2. Data resources and integration/combination methods.

| Name of Model | Methods |
|-------------------|---|
| GTVnp_RD | Integration of radiomics and dosiomics GTVnp data before feature selection |
| GTVnp_R_CECTcT1T2 | Integration of radiomics GTVnp data from CECT, cT1WI, T2WI before feature selection |
| GTVnp_R_CECTcT1 | Integration of radiomics GTVnp data from CECT and cT1WI before feature selection |
| GTVnp_R_cT1T2 | Integration of radiomics GTVnp data from cT1WI and T2WI before feature selection |
| GTVnp_R_cT1 | Single radiomics data from CT1WI |
| GTVnp_R_CECT | Single radiomics data from CECT |
| GTVnp_R_T2 | Single radiomics data from T2WI |
| GTVnp_D | Single dosiomics data from GTVnp |
| GTVn_RD | Integration of radiomics and dosiomics data from GTVn before feature selection |
| GTVn_R | Single radiomics data from GTVn |
| GTVn_D | Single dosiomics data from GTVn |
| PTVn_D | Integration of 60 and 70 Gy dosiomics data before feature selection |
| PTVn_60Gy_D | Single dosiomics data from PTVn_60Gy |
| PTVn_70Gy_D | Single dosiomics data from PTVn_70Gy |
| R | Integration of all radiomics data before feature selection |
| D | Integration of all dosiomics data before feature selection |
| C | Single clinical data |
| C&D | Combine selected clinical and dosiomics data for modeling |
| C&R | Combine selected clinical and radiomics data for modeling |
| RD | Integration of radiomics and dosiomics data before feature selection |
| C&RD | Combine selected clinical and RD data for modeling |
| C>Vnp RD | Combine selected clinical and GTVnp RD data for modeling |
| R&D | Combine selected radiomics and dosiomics data for modeling |
| C&R&D | Combine selected clinical, radiomics and dosiomics data for modeling |

Shapley Additive Explanations (SHAP), an explainable artificial intelligence (AI)-based tool, was applied for further explanation of feature importance for the model with the best AUC result and specific features [41].

3. Results

3.1. Patient Characteristics

A total of 397 continuous patients were collected based on their final diagnosis with pathological validation. Of these patients, with a median age of 54 (range 26–86 years), 242 were enrolled for further analysis following the inclusion and exclusion criteria (details in Figure A1). All patients were negative for oral mucositis with CTCAE graded 0 before radiation therapy. Univariate analysis results of demographic and clinical characteristics for those patients are listed in Table 3.

Table 3. Demographic and clinical characteristics for all patients.

| Characteristics | AOM < Grade 3 (Mild AOM) | AOM ≥ Grade 3 (Severe AOM) | p Value |
|--------------------------------------|-----------------------------|-------------------------------|---------|
| Total Number | 191 (78.9%) | 51 (21.1%) | |
| Age, mean ± SD, years | 54.89 ± 12.25 | 50.9 ± 10.60 | 0.036 * |
| 18–65 | 149 (61.6%) | 44 (18.1%) | |
| ≥65 | 42 (17.4%) | 7 (2.9%) | 0.192 |
| Gender | | | |
| Male | 135 (55.8%) | 41 (16.9%) | |
| Female | 56 (23.1%) | 10 (4.1%) | 0.167 |
| Treatment | | | 0.004 * |
| RT alone | 27 (11.2%) | 0 | |
| CRT | 164 (67.8%) | 51 (21.1%) | 0.031 * |
| T stage | | | |
| T1 | 15 (6.2%) | 3 (0.1%) | |
| T2 | 8 (3.3%) | 5 (2.1%) | |
| T3 | 137 (56.6%) | 28 (11.6%) | |
| T4 | 31 (12.8%) | 15 (6.2%) | |
| N stage | | | 0.091 |
| N1 | 28 (11.2%) | 1 (0.4%) | |
| N2 | 142 (58.7%) | 45 (18.6%) | |
| N3 | 20 (8.2%) | 5 (2.1%) | |
| Pathology | | | |
| Non-keratinizing squamous cell | 175 (72.3%) | 48 (19.8%) | 0.556 |
| Keratinizing squamous-cell carcinoma | 16 (6.6%) | 3 (1.3%) | 0.487 |
| Past health condition | | | |
| Past health good | 92 (38.0%) | 27 (11.2%) | |
| Basic diseases/cancer | 99 (40.9%) | 24 (9.9%) | 0.545 |
| Allegory of History | | | |
| No known drug allergies | 176 (72.7%) | 46 (19.0%) | |
| Allergy history | 15 (6.2%) | 5 (2.1%) | 0.653 |
| Vision | | | |
| Normal | 189 (78.1%) | 51 (21.1%) | |
| With eye impairment | 2 (0.8%) | 0 | 0.463 |
| Hearing | | | |
| Normal | 186 (76.9%) | 48 (19.8%) | |
| With hearing impairment | 5 (2.1%) | 3 (1.2%) | 0.247 |
| Habits | | | |
| Smoking | 9 (3.7%) | 6 (2.5%) | |
| Non-smoker | 182 (75.2%) | 45 (18.6%) | 0.044 * |
| Drinking | 4 (1.7%) | 1 (0.4%) | |
| No alcohol consumption | 187 (77.3%) | 50 (20.7%) | 0.953 |

Table 3. Cont.

| Characteristics | AOM < Grade 3 (Mild AOM) | AOM ≥ Grade 3 (Severe AOM) | p Value |
|----------------------------|-----------------------------|-------------------------------|---------|
| Height, mean ± SD, cm | 163.4 ± 8.5 | 165.0 ± 8.0 | 0.561 |
| Body weight, mean ± SD, kg | | | |
| 1st week of RT | 63.1 ± 11.9 | 66.2 ± 14.6 | 1.599 |
| 2nd week of RT | 62.0 ± 11.8 | 64.9 ± 14.5 | 1.5 |
| 3rd week of RT | 61.2 ± 11.4 | 63.9 ± 14.1 | 0.116 |
| 4th week of RT | 60.2 ± 11.3 | 62.8 ± 14.0 | 1.418 |
| BMI | | | |
| 1st week of RT | | | |
| <25 | 131 (54.1%) | 32 (13.2%) | |
| ≥25 | 60 (24.8%) | 19 (7.9%) | 0.429 |
| 2nd week of RT | | | |
| <25 | 131 (54.1%) | 51 (21.1%) | |
| ≥25 | 60 (24.8%) | 22 (9.1%) | 0.116 |
| 3rd week of RT | | | |
| <25 | 131 (54.1%) | 31 (12.8%) | |
| ≥25 | 55 (22.7%) | 20 (8.3%) | 0.153 |
| 4th week of RT | | | |
| <25 | 142 (58.7%) | 34 (14.0%) | |
| ≥25 | 49 (20.2%) | 17 (7.0%) | 0.274 |

* $p < 0.05$. All the above data are derived from biopsy-proven primary NPC patients without the existence of distant metastasis or co-existing tumors of other type at diagnosis.

3.2. Feature Extraction and Model Development

3.2.1. Feature Extraction

In this study, a total of 1544 radiomics features, 386 features each for four modalities of imaging, were extracted from raw and LoG-filtered images. A total of 836 dosiomics features (210 for GTVn, 211 for GTVnp, 204 for PTVn_60Gy, and 211 for PTVn_70Gy) were extracted from dose images.

3.2.2. Models

For the clinical data, four variables, including age, RT treatment alone, T stage, and smoking habits, were selected after univariate analysis. The logistic regression (LR) model was established with these variables. T stage and smoking habits had statistical significance in the LR model with a p -value < 0.05 (details in Table 4).

Table 4. Logistic regression results for single clinical data model.

| Variables | p-Value | 95% Confidence Interval | |
|--------------|---------|-------------------------|-----------------|
| | | Lower 95% Bound | Upper 95% Bound |
| Age (18, 65) | 0.802 | 0.345 | 2.274 |
| T | 0.007 * | | |
| T 1 | 0.591 | 0.149 | 2.96 |
| T 2 | 0.069 | 0.881 | 29.854 |
| T 3 | 0.024 * | 0.195 | 0.891 |
| RT alone | 0.998 | 0 | . |
| Smoker | 0.043 * | 1.037 | 10.683 |

* $p < 0.05$.

Radiomics and dosiomics features extracted from various VOIs were put into Mann–Whitney U tests and RF classifier step by step. RF selection results of the threshold and feature numbers are listed in Table A3.

Nine categories of single-modal models (C, PTVn_70Gy_D, PTVn_60Gy_D, GTVn_D, GTVnp_D, GTVn_R, GTVnp_R_T2, GTVnp_R_CECT, and GTVnp_R_cT1) were established

with single modal, single modality, and single VOI data. The best validation AUC was at 0.75 ± 0.12 (training AUC = 0.73 ± 0.01) of a GNB model (GTVnp_R_cT1) with radiomics data from GTVnp of cT1WI. Seven groups of models with data integrated before feature selection (raw-data integration) were generated with the best AUC of a GNB model (GTVnp_RD) at 0.81 ± 0.01 (training AUC = 0.79 ± 0.01). This best-performing model was constructed with features selected from radiomics and dosiomics data in the region of GTVnp. In addition, six sets of combined data after feature selection were also used for modeling. A best LR model (C&R&D) with AUC at 0.79 ± 0.14 (training AUC = 0.81 ± 0.02) was set with the simply combined data of selected clinical, dosiomics, and radiomics features (details of mean 10-fold validation AUC results are listed in Figure 3).

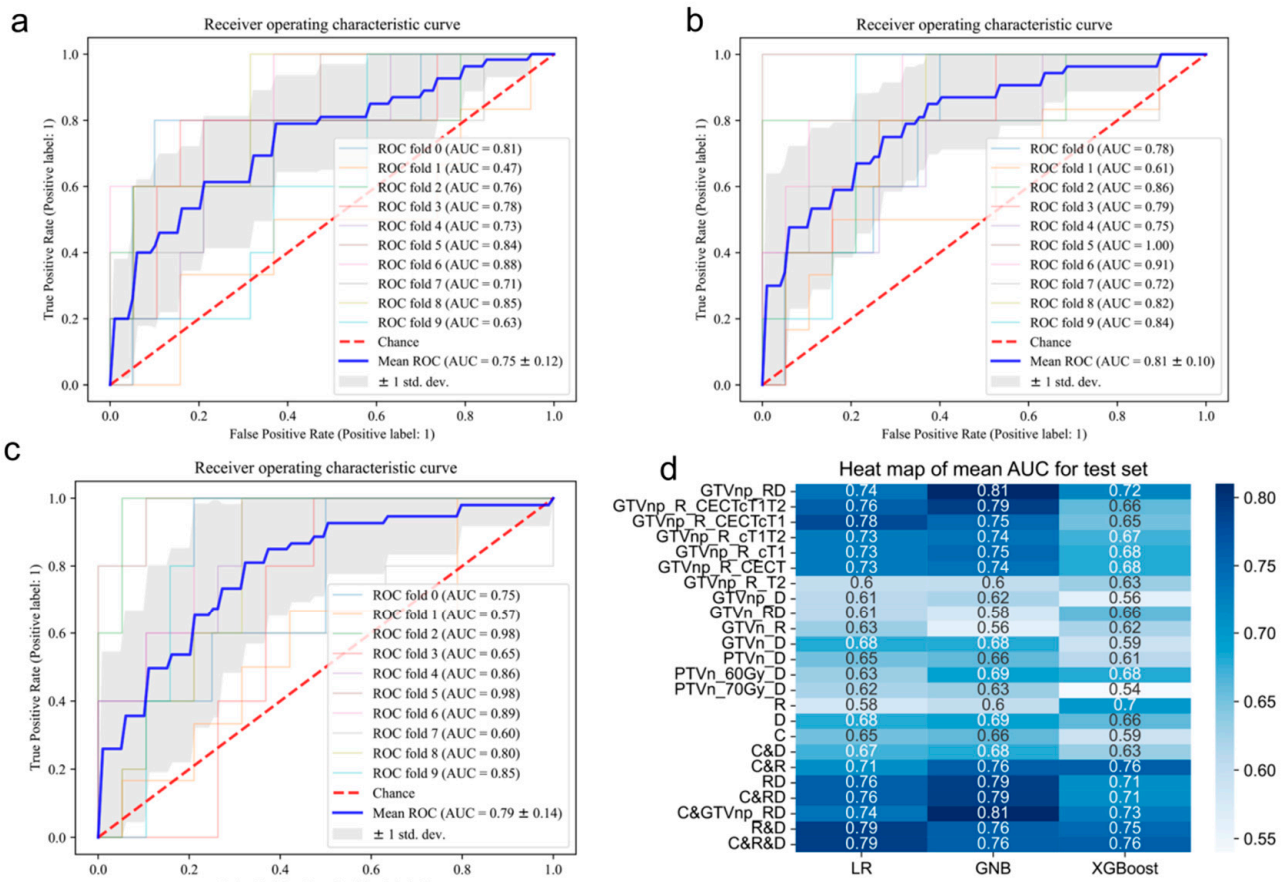


Figure 3. 10-fold validation AUC results for the test set. (a) The AUC plot of GNB model for the GTVnp_R_cT1 data set. (b) The AUC plot of GNB model for the GTVnp_RD data set. (c) The AUC plot of LR model for the C&R&D data set. (d) The heatmap of mean AUC results for all models.

The SHAP analysis showed the importance of the five features in the GTVnp_RD model for prediction of severe AOM. Four of the five features were derived from cT1WI. All five features are texture features. No dosiomics features were selected after the feature selections (details in Figure 4).

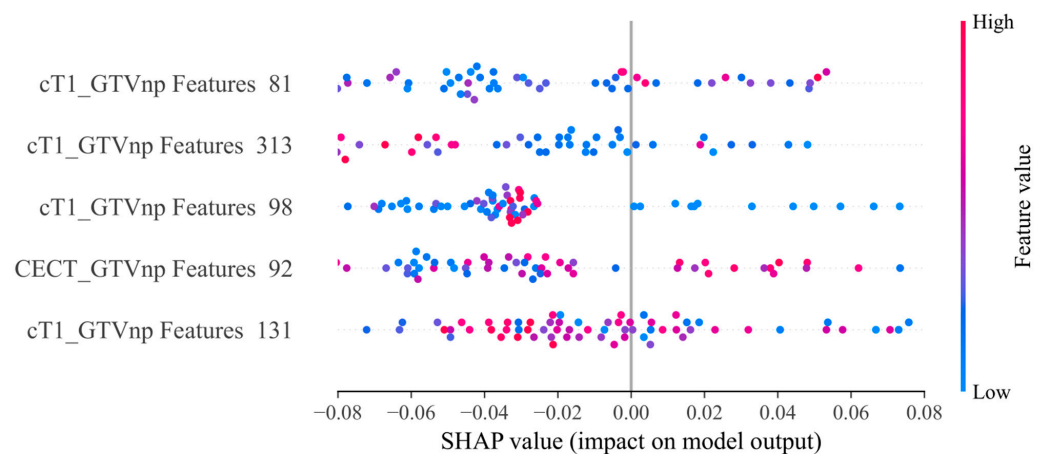


Figure 4. Feature importance of SHAP for XGBoost model of GTVnp_RD. From the highest to the lowest level, the features are categorized in GLSZM, log sigma 60 mm 3D GLCM, original GLDM, GLDM, and log sigma 10 mm 3D GLCM.

4. Discussion

In our study, we used simply combined and data-fusion methods to manage multimodalities of data (clinical, radiomics, and dosiomics), multimodalities of imaging (CECT, cT1WI, and T2WI), and multi-regional information (GTVn, GTVnp, and PTVn) to predict the incidence of severe AOM. Multiple models were established to evaluate and determine which method was effective for clinical decision-making. Comparison of the AUC between models showed that the simple combination of single-modal data of selected features had the most stable performance (C&R&D), with an average AUC of 0.77 ± 0.17 . In addition, data-fusion methods, integrating radiomics and dosiomics data before selection procedures, resulted in the best-performing model (GTVnp_RD), with the best test AUC of 0.81 ± 0.01 . This is also the best AUC among the existing AOM prediction models from previous studies.

The feature numbers in the C&R&D model and GTVnp RD were 29 and 5, respectively. Obviously, data fusion was more efficient for training a model with one-sixth the number of features to achieve stronger model predictability. To better explain the correlations of the selected features and severe AOM for NPC patients, a SHAP plot was applied for the GTVnp_RD XGBoost model. In this model, radiomics features extracted from GTVnp in cT1WI images yielded the highest and majority prediction value for severe AOM.

Poolakkad and his colleagues established a machine learning (ML) model of 253 H&N patients' clinical data with the best AUC of 0.79 for AOM prediction [42]. Most clinical data selected in their study were late after the CRT scheme, for example, the anti-neoplastic chemotherapy-induced pancytopenia, co-morbidity score, and agranulocytosis. It is worth noting that the features and variables selected in our study were all from the data collected before implementation of the RT regimen. Clinicians could predict the severe AOM before the commencement of RT planning. Personalized treatment strategies adjustment could be achieved using the developed prediction model.

Strictly speaking, the concept of dosiomics is originated from radiomics. The data for dosiomics and radiomics are similar in terms of the feature calculation algorithm [43]. The clinical data are different from the “-omics” data in nature. Therefore, instead of integrating raw clinical data with other data, the combination of selected clinical data was only applied in this study. Compared with less increase of AUC for the combination of clinical data with integrated RD data, the clinical data could enhance the prediction capability of single-modal models. The single radiomics models (R) and single clinical models (C) have limited prediction performance with average AUC of three models (LR, GNB, and XGBoost) at 0.63 ± 0.06 and 0.63 ± 0.64 , respectively. When combining the clinical data with the selected radiomics features, the model (C&R) outperformed both R and C models with average AUC at 0.74 ± 0.03 .

The single dosiomics models yielded poor performance, with most AUCs under 0.7 in the validation data set. In a previous study, dose distribution correlated with the incidence and severity of AOM [44]. Dean et al. [45] developed an RF model with a testing AUC of 0.71 ± 0.09 , using a dose–volume histogram, spatial dose metrics from the oral cavity, and clinical data. In the current study, the best dosiomics model had the mean testing AUC of 0.69 ± 0.14 . Different tumor-related VOIs may present different prediction value for severe AOM. The difference in VOI selection between the two studies might shed some light on the discrepancy in the findings. The oral cavity directly represents the dose distribution in the oral mucosa, which might be more accurate than the GTVn, GTVnp, PTVn 60 Gy, or PTVn 70 Gy. The VOI of the oral cavity requires specific contouring. It is worth noting that contouring of the oral cavity is not a common practice in the participating hospital of this study. Extra contouring is labor-intensive work in daily clinical practice. Our study only selected the routine VOI broadly used for RT planning, which could support our model to be applied from bench to bedside for clinical decision-making. Besides, the DVH is prone to over-simplifying the dose distribution [46]. It is recommended to combine or integrate dosiomics data with other modalities of data. When incorporating dosiomics data with other data types, the best mean validation AUC could surge to 0.81 ± 0.01 .

At present, there exists no effective preventive measures for the occurrence of severe AOM in NPC patients undergoing RT. Nevertheless, it is feasible to mitigate the severity of this affliction: (1) Use of alternative radiation techniques, such as proton therapy, may be considered to reduce the risk of oral mucositis while maintaining treatment efficacy [34,47]. (2) Shortening the duration of chemotherapy. For advanced NPC patients who need to accept both radiotherapy and chemotherapy, shortening the exposition time to chemotherapy agents has shown lower mucosal toxicity [48]. (3) Photobiomodulation is a supportive treatment for the protection of high-risk mucositis patients [49]. (4) Supportive care interventions: preemptive or proactive use of supportive care interventions, such as oral hygiene measures, pain management, or nutritional support, may be considered to prevent or reduce the severity of AOM [50].

The limitations of our study were: (1) The mucositis grade levels of our patients had an imbalanced distribution. This might have had a negative influence on the data analysis work. The imbalanced results were the nature of the clinical situation. Patients were stratified into the training and validation groups according to the severity of OM, which could offset the imbalance problem [18,19,34]. (2) Potential bias of smoking information: in our study, the number of smoking patients might be underestimated due to the nature of this patient-reported outcome. This data were reported by patients at the time of their hospital visit and recorded in the nursing consultation notes. (3) The severity of AOM was scaled with standard terminology criteria for adverse events (CTCAE) in v3 or v4.03, almost equivalent to mucositis. Various criteria are available for mucositis grading, such as the those of the Radiation Therapy Oncology Group (RTOG) and the World Health Organization (WHO). These scales have excellent concordance with bundled scores of 3 and 4 to describe severe AOM [51]. The CTCAE is easily conducted by clinicians and nurses and broadly applied in the hospital. (4) The correlations of contributors under AOM for NPC patients are complex. For clinical decision-making, genome information, other clinical information such as fermented-food consumption and EBV infection, and pathological image may also play critical roles. The limited data resources for multimodal data integration are common challenges in the data-mining field. The radiomics data in our study also provided relevant genomic information. Compared with gene test results, the CECT and MRI examination images collected in our research are clinical routines used by clinicians to set the RT plan for NPC patients. These noninvasive examinations could serve as high-throughput screening tools for further application of severe AOM prediction in the future. (5) Other selection of VOIs: for practical consideration, we have not added the VOIs of the oral cavity, tongue, pharyngeal muscles, etc., which may hold potential predictive value for AOM. Further investigation is recommended to incorporate this information to enhance the accuracy of the analysis.

5. Conclusions

AOM is a challenging and distressing complication in NPC patients following RT. Prediction of severe AOM is necessary for timely prevention and intervention, which would further improve the QoL and survival of patients. In this study, we adopted multimodal data (clinical, radiomics, and dosiomics), multimodality of imaging (CECT, cT1WI, and T2WI), and multi-regional information (GTVn, GTVnp, and PTVn) to develop a best-performance model for severe AOM prediction. The simple combination of selected information and data fusion were applied in our work. The results demonstrated that the fusion of radiomics and dosiomics data from the primary tumor could generate the most effective and best-performing model (mean AUC = 0.81 ± 0.01). The data resources and VOIs selected in this study are routinely used in clinical practice, which has excellent potential for further clinical support. Further validation work on a large cohort is warranted to validate model generalizability.

Author Contributions: Conceptualization, Y.D. and S.L.; methodology, Y.D., J.Z. and J.C. (Jing Cao); software, Y.D. and J.Z.; validation, Y.D. and J.Z.; formal analysis, Y.D.; investigation, Y.D., J.Z., X.Z., X.T. and X.H.; resources, F.K.L., C.W.Y., K.A. and J.C. (Jing Cai); data curation, Y.D. and J.Z.; writing—original draft preparation, Y.D.; writing—review and editing, Y.D., S.L., A.L., Y.Z., X.T., H.L. and J.C. (Jing Cai); visualization, Y.D. and J.Z.; supervision, J.C. (Jing Cai); project administration, S.L. and J.C. (Jing Cai); funding acquisition, J.C. (Jing Cai). All authors have read and agreed to the published version of the manuscript.

Funding: This research was partly supported by research grants of Shenzhen Basic Research Program (JCYJ20210324130209023), Shenzhen-Hong Kong-Macau S&T Program (Category C) (SGDX20201103095002019), Mainland-Hong Kong Joint Funding Scheme (MHKJFS) (MHP/005/20), Project of Strategic Importance Fund (P0035421) and Projects of RISA (P0043001) from The Hong Kong Polytechnic University.

Institutional Review Board Statement: Ethical review and approval were waived for this study due to the natural of retrospective study.

Informed Consent Statement: Patient consent was waived due to the nature of the retrospective study.

Data Availability Statement: For patients' privacy protection, the data availability was not applicable.

Acknowledgments: Thanks to Qi Liu for general support with the initial data analysis.

Conflicts of Interest: The authors declare no conflict of interest.

Appendix A

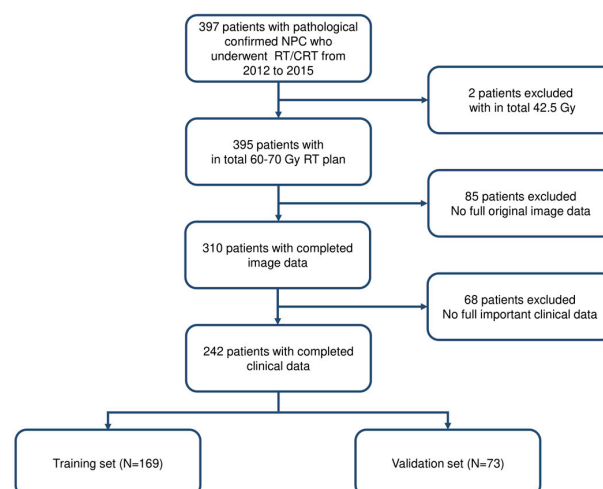


Figure A1. Schematic diagram of patient selection.

Appendix B

CECT. All patients were scanned in the CT stimulator (16-slice Brilliance Big 1Bore CT, Philips Medical Systems, Cleveland, OH) at Queen Elizabeth Hospital in Hong Kong. The scanned regions were from vertex to 5 cm below the sternoclavicular notch. The contrast-enhanced images were acquired at 30 s after intravenous injection of 70 mL iodinated contrast agents. The detailed acquisition parameters are listed in Table A1.

Table A1. Acquisition parameters of CECT.

| Parameters | CECT |
|----------------------|-----------|
| Pitch | 1 |
| Kilovoltage (kV) | 120 |
| Current (mAs) | 250–350 |
| Slice thickness (mm) | 3 |
| Matrix | 512 × 512 |
| Scan time (s) | 15 |

MRI. MRI scans were acquired with an MR scanner (1.5 Tesla, Siemens Avanto, Germany). T2 weighted imaging with short-tau-inversion-recovery (STIR) sequence and cT1WI with spin-echo MRI sequence were applied. The detailed acquisition parameters are listed in Table A2.

Table A2. Parameters of T2WI and T1WI.

| Parameters | T2-STIR | cT1WI |
|-------------------------------|-------------------|---------------------|
| [TR]/[TE] (ms) | 7640/97 | 739/17 |
| FOV (cm ²) | 24 × 24 | 24 × 24 |
| Number of acquisitions | 1 | 1 |
| Slice thickness (mm × slices) | 4 × 25 | 3 × 28 |
| Spacing (cm ³) | 0.75 × 0.75 × 4.4 | 0.938 × 0.938 × 3.3 |
| Matrix | 320 × 320 | 256 × 256 |

Appendix C

Table A3. Threshold of RFC selection and feature numbers for further model development.

| Modal of Data | Threshold | Number of Features |
|-------------------|-----------|--------------------|
| GTVnp_RD | 0.014 | 5 |
| GTVnp_R_CECTcT1T2 | 0.01 | 8 |
| GTVnp_R_CECTcT1 | 0.0125 | 5 |
| GTVnp_R_cT1T2 | 0.125 | 5 |
| GTVnp_R_cT1 | 0.015 | 4 |
| GTVnp_R_CECT | 0.01 | 19 |
| GTVnp_R_T2 | 0.03 | 2 |
| GTVnp_D | 0.024 | 6 |
| GTVn_RD | 0.02 | 7 |
| GTVn_R | 0.03 | 7 |
| GTVn_D | 0.06 | 7 |
| PTVn_D | 0.03 | 3 |
| PTVn_60Gy_D | 0.03 | 12 |
| PTVn_70Gy_D | 0.042 | 1 |
| R | 0.012 | 2 |
| D | 0.016 | 13 |
| RD | 0.005 | 13 |

Appendix D

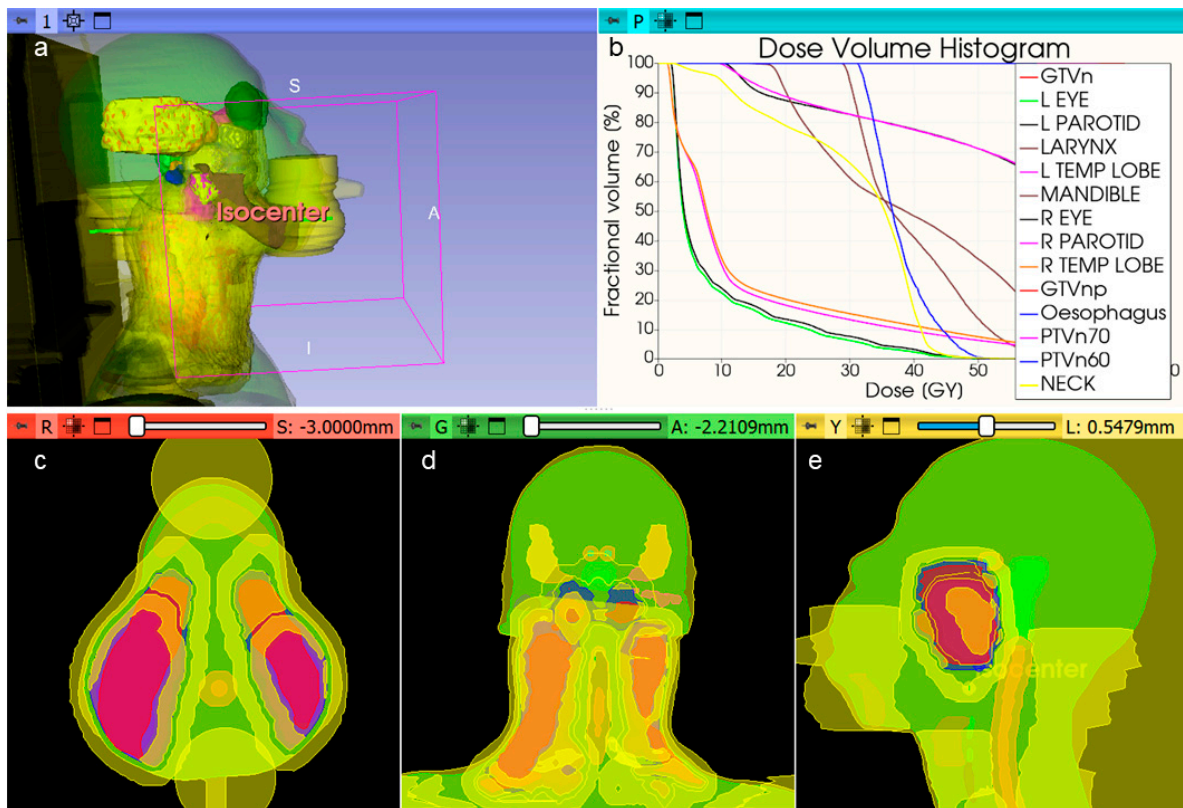


Figure A2. Dose maps of NPC patients undergoing IMRT. (a) 3D view of NPC patient. (b) DVH of multiple VOIs. (c). Axial view of patient in different VOIs. (d). Coronal view of patient. (e). Sagittal view of patient.

References

- Chen, Y.-P.; Chan, A.T.C.; Le, Q.-T.; Blanchard, P.; Sun, Y.; Ma, J. Nasopharyngeal carcinoma. *Lancet* **2019**, *394*, 64–80. [[CrossRef](#)] [[PubMed](#)]
- Chang, E.T.; Ye, W.; Zeng, Y.-X.; Adami, H.-O. The Evolving Epidemiology of Nasopharyngeal Carcinoma. *Cancer Epidemiol. Biomarkers Prev.* **2021**, *30*, 1035–1047. [[CrossRef](#)] [[PubMed](#)]
- Chen, Y.-P.; Ismaila, N.; Chua, M.L.K.; Colevas, A.D.; Haddad, R.; Huang, S.H.; Wee, J.T.S.; Whitley, A.C.; Yi, J.-L.; Yom, S.S.; et al. Chemotherapy in Combination with Radiotherapy for Definitive-Intent Treatment of Stage II-IVA Nasopharyngeal Carcinoma: CSCO and ASCO Guideline. *J. Clin. Oncol.* **2021**, *39*, 840–859. [[CrossRef](#)]
- Bossi, P.; Chan, A.; Licitra, L.; Trama, A.; Orlandi, E.; Hui, E.; Halámková, J.; Mattheis, S.; Baujat, B.; Hardillo, J.; et al. Nasopharyngeal carcinoma: ESMO-EURACAN Clinical Practice Guidelines for diagnosis, treatment and follow-up. *Ann. Oncol.* **2020**, *32*, 452–465. [[CrossRef](#)]
- You, R.; Liu, Y.-P.; Huang, P.-Y.; Zou, X.; Sun, R.; He, Y.-X.; Wu, Y.-S.; Shen, G.-P.; Zhang, H.-D.; Duan, C.-Y.; et al. Efficacy and Safety of Locoregional Radiotherapy with Chemotherapy vs Chemotherapy Alone in De Novo Metastatic Nasopharyngeal Carcinoma: A Multicenter Phase 3 Randomized Clinical Trial. *JAMA Oncol.* **2020**, *6*, 1345. [[CrossRef](#)]
- Tang, L.-L.; Guo, R.; Zhang, N.; Deng, B.; Chen, L.; Cheng, Z.-B.; Huang, J.; Hu, W.-H.; Huang, S.H.; Luo, W.-J.; et al. Effect of Radiotherapy Alone vs Radiotherapy with Concurrent Chemoradiotherapy on Survival Without Disease Relapse in Patients with Low-risk Nasopharyngeal Carcinoma: A Randomized Clinical Trial. *JAMA* **2022**, *328*, 728–736. [[CrossRef](#)]
- Wang, K.; Tepper, J.E. Radiation therapy-associated toxicity: Etiology, management, and prevention. *CA A Cancer J. Clin.* **2021**, *71*, 437–454. [[CrossRef](#)]
- Elad, S.; Yarom, N.; Zadik, Y.; Kuten-Shorrer, M.; Sonis, S.T. The broadening scope of oral mucositis and oral ulcerative mucosal toxicities of anticancer therapies. *CA A Cancer J. Clin.* **2021**, *72*, 57–77. [[CrossRef](#)]
- Raber-Durlacher, J.E.; Elad, S.; Barasch, A. Oral mucositis. *Oral Oncol.* **2010**, *46*, 452–456. [[CrossRef](#)] [[PubMed](#)]
- McDowell, L.; Corry, J.; Ringash, J.; Rischin, D. Quality of Life, Toxicity and Unmet Needs in Nasopharyngeal Cancer Survivors. *Front. Oncol.* **2020**, *10*, 930. [[CrossRef](#)] [[PubMed](#)]

11. Li, H.; You, Y.; Lin, C.; Zheng, M.; Hong, C.; Chen, J.; Li, D.; Au, W.W.; Chen, Z. XRCC1 codon 399Gln polymorphism is associated with radiotherapy-induced acute dermatitis and mucositis in nasopharyngeal carcinoma patients. *Radiat. Oncol.* **2013**, *8*, 31. [[CrossRef](#)]
12. Yang, D.-W.; Wang, T.-M.; Zhang, J.-B.; Li, X.-Z.; He, Y.-Q.; Xiao, R.; Xue, W.-Q.; Zheng, X.-H.; Zhang, P.-F.; Zhang, S.-D.; et al. Genome-wide association study identifies genetic susceptibility loci and pathways of radiation-induced acute oral mucositis. *J. Transl. Med.* **2020**, *18*, 1–12. [[CrossRef](#)]
13. Orlandi, E.; Iacovelli, N.A.; Rancati, T.; Cicchetti, A.; Bossi, P.; Pignoli, E.; Bergamini, C.; Licitra, L.; Fallai, C.; Valdagni, R.; et al. Multivariable model for predicting acute oral mucositis during combined IMRT and chemotherapy for locally advanced nasopharyngeal cancer patients. *Oral Oncol.* **2018**, *86*, 266–272. [[CrossRef](#)]
14. Inada, M.; Nishimura, Y.; Ishikura, S.; Ishikawa, K.; Murakami, N.; Kodaira, T.; Ito, Y.; Tsuchiya, K.; Murakami, Y.; Saito, J.; et al. Organs-at-risk dose constraints in head and neck intensity-modulated radiation therapy using a dataset from a multi-institutional clinical trial (JCOG1015A1). *Radiat. Oncol.* **2022**, *17*, 1–8. [[CrossRef](#)] [[PubMed](#)]
15. Xu, T.; Liu, Y.; Dou, S.; Li, F.; Guan, X.; Zhu, G. Weekly cetuximab concurrent with IMRT aggravated radiation-induced oral mucositis in locally advanced nasopharyngeal carcinoma: Results of a randomized phase II study. *Oral Oncol.* **2015**, *51*, 875–879. [[CrossRef](#)] [[PubMed](#)]
16. Köstler, W.J.; Hejna, M.; Wenzel, C.; Zielinski, C.C. Oral Mucositis Complicating Chemotherapy and/or Radiotherapy: Options for Prevention and Treatment. *CA A Cancer J. Clin.* **2001**, *51*, 290–315. [[CrossRef](#)]
17. Scully, C.; Epstein, J.; Sonis, S. Oral mucositis: A challenging complication of radiotherapy, chemotherapy, and radiochemotherapy: Part 1, pathogenesis and prophylaxis of mucositis. *Head Neck* **2003**, *25*, 1057–1070. [[CrossRef](#)] [[PubMed](#)]
18. Shu, Z.; Zeng, Z.; Yu, B.; Huang, S.; Hua, Y.; Jin, T.; Tao, C.; Wang, L.; Cao, C.; Xu, Z.; et al. Nutritional Status and Its Association with Radiation-Induced Oral Mucositis in Patients with Nasopharyngeal Carcinoma During Radiotherapy: A Prospective Study. *Front. Oncol.* **2020**, *10*, 594687. [[CrossRef](#)]
19. Elting, L.S.; Cooksley, C.D.; Chambers, M.S.; Garden, A.S. Risk, Outcomes, and Costs of Radiation-Induced Oral Mucositis Among Patients with Head-and-Neck Malignancies. *Int. J. Radiat. Oncol. Biol. Phys.* **2007**, *68*, 1110–1120. [[CrossRef](#)]
20. Saito, N.; Imai, Y.; Muto, T.; Sairenchi, T. Low body mass index as a risk factor of moderate to severe oral mucositis in oral cancer patients with radiotherapy. *Support. Care Cancer* **2012**, *20*, 3373–3377. [[CrossRef](#)]
21. Rosenthal, D.I.; Trotti, A. Strategies for Managing Radiation-Induced Mucositis in Head and Neck Cancer. *Semin. Radiat. Oncol.* **2009**, *19*, 29–34. [[CrossRef](#)]
22. Chong, V.; Ong, C. Nasopharyngeal carcinoma. *Eur. J. Radiol.* **2008**, *66*, 437–447. [[CrossRef](#)]
23. Xia, P.; Fu, K.K.; Wong, G.W.; Akazawa, C.; Verhey, L.J. Comparison of treatment plans involving intensity-modulated radiotherapy for nasopharyngeal carcinoma. *Int. J. Radiat. Oncol.* **2000**, *48*, 329–337. [[CrossRef](#)] [[PubMed](#)]
24. Lahat, D.; Adali, T.; Jutten, C. Multimodal data fusion: An overview of methods, challenges, and prospects. *Proc. IEEE* **2015**, *103*, 1449–1477. [[CrossRef](#)]
25. Boehm, K.M.; Khosravi, P.; Vanguri, R.; Gao, J.; Shah, S.P. Harnessing multimodal data integration to advance precision oncology. *Nat. Rev. Cancer* **2021**, *22*, 114–126. [[CrossRef](#)] [[PubMed](#)]
26. Lipkova, J.; Chen, R.J.; Chen, B.; Lu, M.Y.; Barbieri, M.; Shao, D.; Vaidya, A.J.; Chen, C.; Zhuang, L.; Williamson, D.F.; et al. Artificial intelligence for multimodal data integration in oncology. *Cancer Cell* **2022**, *40*, 1095–1110. [[CrossRef](#)]
27. Teng, X.; Zhang, J.; Ma, Z.; Zhang, Y.; Lam, S.; Li, W.; Xiao, H.; Li, T.; Li, B.; Zhou, T.; et al. Improving radiomic model reliability using robust features from perturbations for head-and-neck carcinoma. *Front. Oncol.* **2022**, *12*, 974467. [[CrossRef](#)]
28. Lam, S.-K.; Zhang, Y.; Zhang, J.; Li, B.; Sun, J.-C.; Liu, C.Y.-T.; Chou, P.-H.; Teng, X.; Ma, Z.-R.; Ni, R.-Y.; et al. Multi-Organ Omics-Based Prediction for Adaptive Radiation Therapy Eligibility in Nasopharyngeal Carcinoma Patients Undergoing Concurrent Chemoradiotherapy. *Front. Oncol.* **2022**, *11*, 792024. [[CrossRef](#)] [[PubMed](#)]
29. Zhang, Y.; Lam, S.; Yu, T.; Teng, X.; Zhang, J.; Lee, F.K.-H.; Au, K.-H.; Yip, C.W.-Y.; Wang, S.; Cai, J. Integration of an imbalance framework with novel high-generalizable classifiers for radiomics-based distant metastases prediction of advanced nasopharyngeal carcinoma. *Knowl.-Based Syst.* **2021**, *235*, 107649. [[CrossRef](#)]
30. Li, B.; Zheng, X.; Zhang, J.; Lam, S.; Guo, W.; Wang, Y.; Cui, S.; Teng, X.; Zhang, Y.; Ma, Z.; et al. Lung Subregion Partitioning by Incremental Dose Intervals Improves Omics-Based Prediction for Acute Radiation Pneumonitis in Non-Small-Cell Lung Cancer Patients. *Cancers* **2022**, *14*, 4889. [[CrossRef](#)]
31. Li, B.; Ren, G.; Guo, W.; Zhang, J.; Lam, S.-K.; Zheng, X.; Teng, X.; Wang, Y.; Yang, Y.; Dan, Q.; et al. Function-Wise Dual-Omics analysis for radiation pneumonitis prediction in lung cancer patients. *Front. Pharmacol.* **2022**, *13*, 971849. [[CrossRef](#)]
32. Hansen, C.; Bertelsen, A.; Zukauskaitė, R.; Johnsen, L.; Bernchou, U.; Thwaites, D.; Eriksen, J.; Johansen, J.; Brink, C. Prediction of radiation-induced mucositis of H&N cancer patients based on a large patient cohort. *Radiother. Oncol.* **2020**, *147*, 15–21. [[CrossRef](#)]
33. Li, P.-J.; Li, K.-X.; Jin, T.; Lin, H.-M.; Fang, J.-B.; Yang, S.-Y.; Shen, W.; Chen, J.; Zhang, J.; Chen, X.-Z.; et al. Predictive Model and Precaution for Oral Mucositis During Chemo-Radiotherapy in Nasopharyngeal Carcinoma Patients. *Front. Oncol.* **2020**, *10*, 596822. [[CrossRef](#)] [[PubMed](#)]
34. Dodd, M.J.; Miaskowski, C.; Shiba, G.H.; Dibble, S.L.; Greenspan, D.; MacPhail, L.; Paul, S.M.; Larson, P. Risk factors for chemotherapy-induced oral mucositis: Dental appliances, oral hygiene, previous oral lesions, and history of smoking. *Cancer Investig.* **1999**, *17*, 278–284. [[CrossRef](#)]

35. Zwanenburg, A.; Vallières, M.; Abdalah, M.A.; Aerts, H.J.W.L.; Andrearczyk, V.; Apte, A.; Ashrafinia, S.; Bakas, S.; Beukinga, R.J.; Boellaard, R.; et al. The Image Biomarker Standardization Initiative: Standardized Quantitative Radiomics for High-Throughput Image-based Phenotyping. *Radiology* **2020**, *295*, 328–338. [[CrossRef](#)]
36. van Griethuysen, J.J.M.; Fedorov, A.; Parmar, C.; Hosny, A.; Aucoin, N.; Narayan, V.; Beets-Tan, R.G.H.; Fillion-Robin, J.-C.; Pieper, S.; Aerts, H.J.W.L. Computational Radiomics System to Decode the Radiographic Phenotype. *Cancer Res.* **2017**, *77*, e104–e107. [[CrossRef](#)]
37. Lowekamp, B.C.; Chen, D.T.; Eibanez, L.; Eblezek, D. The Design of SimpleITK. *Front. Neuroinform.* **2013**, *7*, 45. [[CrossRef](#)] [[PubMed](#)]
38. Grégoire, V.; Levendag, P.; Ang, K.K.; Bernier, J.; Braaksmā, M.; Budach, V.; Chao, C.; Coche, E.; Cooper, J.S.; Cosnard, G.; et al. CT-based delineation of lymph node levels and related CTVs in the node-negative neck: DAHANCA, EORTC, GORTEC, NCIC, RTOG consensus guidelines. *Radiother. Oncol.* **2003**, *69*, 227–236. [[CrossRef](#)]
39. Gabryś, H.S.; Buettner, F.; Sterzing, F.; Hauswald, H.; Bangert, M. Design and Selection of Machine Learning Methods Using Radiomics and Dosiomics for Normal Tissue Complication Probability Modeling of Xerostomia. *Front. Oncol.* **2018**, *8*, 35. [[CrossRef](#)]
40. Buettner, F.; Miah, A.B.; Gulliford, S.L.; Hall, E.; Harrington, K.J.; Webb, S.; Partridge, M.; Nutting, C.M. Novel approaches to improve the therapeutic index of head and neck radiotherapy: An analysis of data from the PARSPORT randomised phase III trial. *Radiother. Oncol.* **2012**, *103*, 82–87. [[CrossRef](#)] [[PubMed](#)]
41. Lundberg, S.M.; Lee, S.I. A unified approach to interpreting model predictions. *Adv. Neural Inf. Process. Syst.* **2017**, *30*. [[CrossRef](#)]
42. Satheeshkumar, P.S.; El-Dallal, M.; Mohan, M.P. Feature selection and predicting chemotherapy-induced ulcerative mucositis using machine learning methods. *Int. J. Med. Inform.* **2021**, *154*, 104563. [[CrossRef](#)] [[PubMed](#)]
43. Rossi, L.; Bijman, R.; Schillemans, W.; Aluwini, S.; Cavedon, C.; Witte, M.; Incrocci, L.; Heijmen, B. Texture analysis of 3D dose distributions for predictive modelling of toxicity rates in radiotherapy. *Radiother. Oncol.* **2018**, *129*, 548–553. [[CrossRef](#)] [[PubMed](#)]
44. Sanguineti, G.; Sormani, M.P.; Marur, S.; Gunn, G.B.; Rao, N.; Cianchetti, M.; Ricchetti, F.; McNutt, T.; Wu, B.; Forastiere, A. Effect of Radiotherapy and Chemotherapy on the Risk of Mucositis During Intensity-Modulated Radiation Therapy for Oropharyngeal Cancer. *Int. J. Radiat. Oncol.* **2012**, *83*, 235–242. [[CrossRef](#)] [[PubMed](#)]
45. Dean, J.A.; Wong, K.H.; Welsh, L.C.; Jones, A.-B.; Schick, U.; Newbold, K.L.; Bhide, S.A.; Harrington, K.J.; Nutting, C.M.; Gulliford, S.L. Normal tissue complication probability (NTCP) modelling using spatial dose metrics and machine learning methods for severe acute oral mucositis resulting from head and neck radiotherapy. *Radiother. Oncol.* **2016**, *120*, 21–27. [[CrossRef](#)]
46. Giraud, P.; Giraud, P.; Gasnier, A.; El Ayachy, R.; Kreps, S.; Foy, J.-P.; Durdux, C.; Huguet, F.; Burgun, A.; Bibault, J.-E. Radiomics and Machine Learning for Radiotherapy in Head and Neck Cancers. *Front. Oncol.* **2019**, *9*, 174. [[CrossRef](#)]
47. Moreno, A.C.; Frank, S.J.; Garden, A.S.; Rosenthal, D.I.; Fuller, C.D.; Gunn, G.B.; Reddy, J.P.; Morrison, W.H.; Williamson, T.D.; Holliday, E.B.; et al. Intensity modulated proton therapy (IMPT)–The future of IMRT for head and neck cancer. *Oral Oncol.* **2019**, *88*, 66–74. [[CrossRef](#)]
48. Plevová, P. Prevention and treatment of chemotherapy- and radiotherapy-induced oral mucositis: A review. *Oral Oncol.* **1999**, *35*, 453–470. [[CrossRef](#)]
49. Melo, W.W.P.; Aragão, W.A.B.; Baia-Da-Silva, D.C.; Nascimento, P.C.; Lima, R.R.; de Souza-Rodrigues, R.D. Effects of Photo-biomodulation on Oral Mucositis: Visualization and Analysis of Knowledge. *Life* **2022**, *12*, 1940. [[CrossRef](#)]
50. Araújo, S.N.M.; Luz, M.H.B.A.; da Silva, G.R.F.; Andrade, E.M.L.R.; Nunes, L.C.C.; Moura, R.O. Cancer patients with oral mucositis: Challenges for nursing care. *Rev. Latino-Am. Enferm.* **2015**, *23*, 267–274. [[CrossRef](#)]
51. Villa, A.; Vollemans, M.; De Moraes, A.; Sonis, S. Concordance of the WHO, RTOG, and CTCv4.0 grading scales for the evaluation of oral mucositis associated with chemoradiation therapy for the treatment of oral and oropharyngeal cancers. *Support. Care Cancer* **2021**, *29*, 6061–6068. [[CrossRef](#)] [[PubMed](#)]

Disclaimer/Publisher’s Note: The statements, opinions and data contained in all publications are solely those of the individual author(s) and contributor(s) and not of MDPI and/or the editor(s). MDPI and/or the editor(s) disclaim responsibility for any injury to people or property resulting from any ideas, methods, instructions or products referred to in the content.